HOKKAIDO UNIVERSITY

Title	Sediment Discharge in Yukon River, Alaska : Its Continuous Measurement and Interpretation
Author(s)	CHIKITA, Kazuhisa; KUMAI, Ryuji; KEMNITZ, Richard T.
Citation	Journal of the Faculty of Science, Hokkaido University. Series 7, Geophysics, 11(4), 691-706
Issue Date	2000-03-24
Doc URL	https://hdl.handle.net/2115/8856
Type	departmental bulletin paper
File Information	11(4)_p691-706.pdf

Hokkaido University Collection of Scholarly and Academic Papers : HUSCAP

Jour. Fac. Sci., Hokkaido Univ., Ser. VII (Geophysics), Vol. 11, No. 4, 691-706, 2000.

Sediment Discharge in Yukon River, Alaska : Its Continuous Measurement and Interpretation

Kazuhisa Chikita, Ryuji Kumai

Division of Earth and Planetary Sciences, Graduate School of Science, Hokkaido University, Sapporo 060-0810, Japan

and

Richard T. Kemnitz

Water Resources Division, Geological Survey, U.S. Department of the Interior, 800 Yukon Dr., University of Alaska Fairbanks, Fairbanks, Alaska 99775-5170, U.S.A.

(Received November 30, 1999)

Abstract

In order to clarify the mechanism of sediment discharge in Yukon River, Alaska, continuous measurements of turbidity and temperature of river water were performed at a site in the middle region of the drainage basin for a period of June to September 1998. Water turbidity recorded at a fixed point represents the crosssectional fluctuation of suspended sediment concentration (SSC) with an error of less than 20 mg/L, exhibiting a one-to-one correspondence between turbidity and SSC. A time series of sediment discharge, the product of SSC and water discharge, was obtained using the turbidity record and water discharge data of U.S. Geological Survey. Sediment discharge of Yukon River seasonally varies with high water discharge and high SSC by snowmelt until early July and subsequently with relatively low water discharge and very high SSC by glacier-melt and rainfall through early September. The snowmelt sediment discharge is probably due to fluvial entrainment of bank sediment in the upstream.

1. Introduction

The monitoring of sediment discharge of a river is important in order to appreciate the deforestation, a nutrient cycle affecting an aquatic environment, and geomorphic processes in a drainage basin. In arctic and subarctic regions such as Alaska and Siberia, sediment discharge could also be an indicator of a global-warming effect on the melt of permafrost. However, there are few continuous measurements of sediment discharge because of a technical problem

for reproducing actual suspended sediment concentration by a turbidimeter (e.g., Clifford et al., 1995; Riley, 1998). Meanwhile, rain-runoff analyses for large rivers are developed in Chao Phraya River, Thailand (Jha et al., 1998) and Mississippi River, U.S.A. (Liston et al., 1994). Any long-term observations of sediment discharge in large rivers, however, have not been performed, and their sediment-discharging mechanism is not yet clear. Sediment transport rate of Tanana River, a tributary of Yukon River, was measured by U.S. Geological Survey (Burrows et al., 1981; Harrold et al., 1983). As a result, the transport rate of suspended sediment proved to be larger than that of bedload by a factor of about 100. Suspended sediment discharge thus seems to prevail in Yukon River. In the present study, a self-recording turbidimeter of infrared ray back-scattering type is deployed for continuous measurement of water turbidity, and an observation error of water turbidity for crosssectional suspended sediment concentration is estimated to numerically obtain a time series of suspended sediment discharge.

2. Study area and methods

Yukon River has the drainage area of 9×10^5 km^2 and the channel length of 3,700 km. Its drainage basin is located on the border of the Arctic Circle, and consists of tundra and forest regions with discontinuous permafrost and high mountain regions with exposed bedrock or glacial cover (Fig. 1). The eastern upstream regions of the drainage basin belong to the Yukon Territory of Canada. The glacial cover is dominant in the Alaska Range with Mt. McKinley (6,194 m asl; above sea level), Mt. Foraker (5,302 m asl), etc., and in Wrangell Mountains and St. Elias Mountains. Tanana River, a tributary of Yukon River, has a large glacier-covered area in the Alaska Range and part of Wrangell Mountains, compared with that in Wrangell and St. Elias Mountains upstream of site EAG. Periglacial landforms such as alas and pingo are developed in the alluvial lowland region around the Yukon River channel. The geology of the drainage basin is mainly alluvium, diluvium, Cambrian, Carboniferous, Cretaceous and Tertiary sedimentary rocks, Silurian, Cretaceous and Quaternary volcanic rocks, and Jurassic and Tertiary intrusive rocks. Mean annual precipitation for 1961 to 1990 is 361 mm at site GLN (Galena, 46 m asl), 277 mm at Fairbanks (138 m asl), 241 mm at site NWY (Northway, 525 m asl), and 269 mm at site WHH (Whitehorse, 703 m), which consist of 54 % rainfall and 46 % snowfall, 35% rainfall and 65 % snowfall, 64 % rainfall and 36 % snowfall, and 59% rainfall and 41% snowfall, respectively (see Fig. 1 for location). The

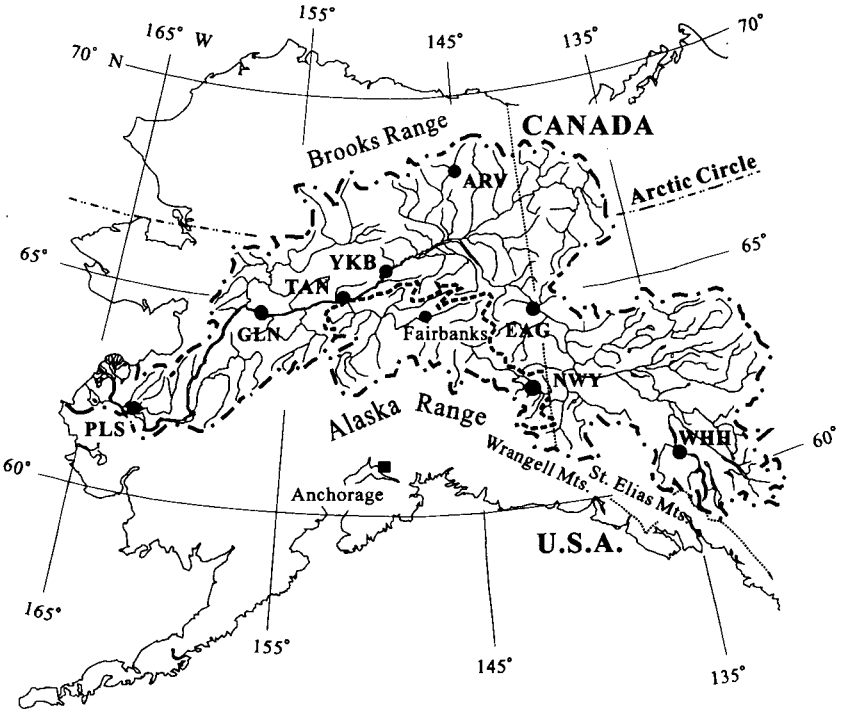

Fig. 1. Location of observation sites (sites YKB and PLS) and representative meteorological stations (sites GLN, TAN, ARV, NWY and WHH) in a drainage basin of Yukon River. River stage and discharge are gauged at site YKB, site EAG and Fairbanks by U.S. Geological Survey. The thick dotted line indicates a water divide of Tanana River.

drainage basin of Yukon River is thus located in an arctic or subarctic, arid region, and its baseflow could be dominated by the melt of underground seasonal ice rather than by the underground storage of precipitated water.

Water levels of Yukon River and its tributary, Tanana River, are measured at 1 h intervals at some stations of U.S. Geological Survey. Of these, at site YKB (Yukon Bridge) in the middle region of Yukon River (Fig. 1), continuous measurements of turbidity and temperature of river water were performed at 2 h and 30 min intervals, respectively for a period of 21 June to 6 September 1998. We measured the turbidity and temperature by a self-recording turbidimeter of infrared ray back-scattering type (Alec Electronics, Inc., Japan, model MTB-16K: accuracy of ± 40 ppm for a range of 0 to 2,000 ppm, resolution of 1 ppm) and a temperature data logger (ONSET Computer, Inc., U.S.A.: accuracy of ± 0.2°C for a range of -5 to 37°C), respectively. Figure 2 shows a

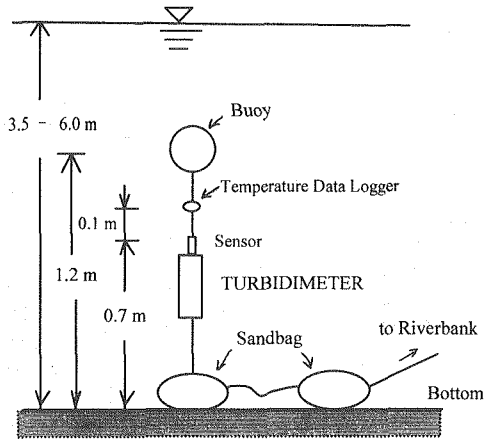

Fig. 2. Mooring system of a self-recording turbidimeter and a temperature data logger at site YKB.

mooring sandbag-buoy system of the turbidimeter and temperature data logger, which were fixed at 0.7 m and 0.8 m above the riverbed, respectively on 21 June. This measuring point was then located at about 50 m off the left bank and downstream of No. 2 Pier of Yukon Bridge. This bridge has 5 piers of No. 2 off the left bank to No. 6 off the right bank, standing every 124 m in transect.

Recorded water turbidity was converted to suspended sediment concentration (SSC ; mg/L) of river water by using a relation between water turbidity and SSC of simultaneously sampled water (Fig. 3). The water samples were

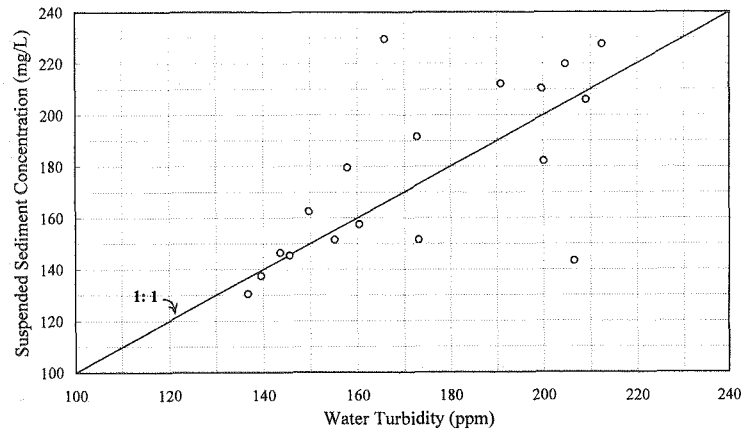

Fig. 3. Relation between vertical mean water turbidity and suspended sediment concentration of depth-integrated water.

obtained in transect of site YKB in 1998 and 1999, using a depth-integrated sampler on a boat, and then filtered with millipore filters of 0.45 μm opening. The resultant SSC was compared with vertical mean turbidity obtained by lowering another turbidimeter of same type at depth intervals of 0.5 m or 1 m on a boat. As a result, the mean turbidity values appear to be reduced to SSC values themselves, i.e., exhibiting a one-to-one correspondence. The scatter of plots in Fig. 3 probably reflects the spatial and temporal fluctuations due to full turbulence of river flow, though each of the vertical turbidity measurements overlapped with correspondent water sampling at less than 5 min.

In order to evaluate an observation error of one-point recorded turbidity for crosssectional SSC, crosssectional fluctuation of vertical SSC profiles was compared with turbidity values simultaneously recorded.

For comparison, turbidity and temperature of river water and air temperature were measured at intervals of 30 min, 30 min, and 1 h, respectively at site PLS near the estuary facing the Bering Sea for a period of 27 to 28 June (Fig. 1). A turbidimeter and a data logger were then fixed at 0.2 m above the riverbed (at a water depth of 0.4 m) at 15 m off the right bank. The turbidity recorded was used as SSC itself, considering their one-to-one correspondence at site YKB. Since water discharge at site PLS has not been measured by U.S. Geological Survey since 1996, we calculated the daily mean discharge from a water level read out once a day by Department of Fish and Game, Anchorage, using a relation about the 1995 data (Fig. 4).

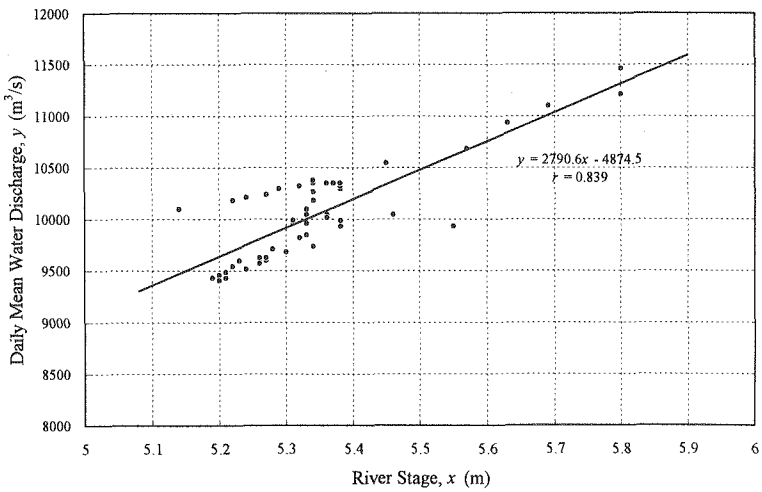

Fig. 4. Relation between water level and daily mean water discharge measured at site PLS in 1995.

In addition to suspended sediment in depth-integrated water, bank sediment was sampled at site YKB and site PLS. Their grain size was analyzed by sieving for grains of $d>44$ μm and by gravitational settling with a centrifuge for those of $d\leqq 44$ μm.

3. Results and discussion

3.1 Observation error of water turbidity

An observation error of water turbidity measured at a fixed point is here estimated in order to appreciate its representation for crosssectional fluctuation of SSC and to numerically obtain a time series of sediment discharge from the representative SSC and water discharge.

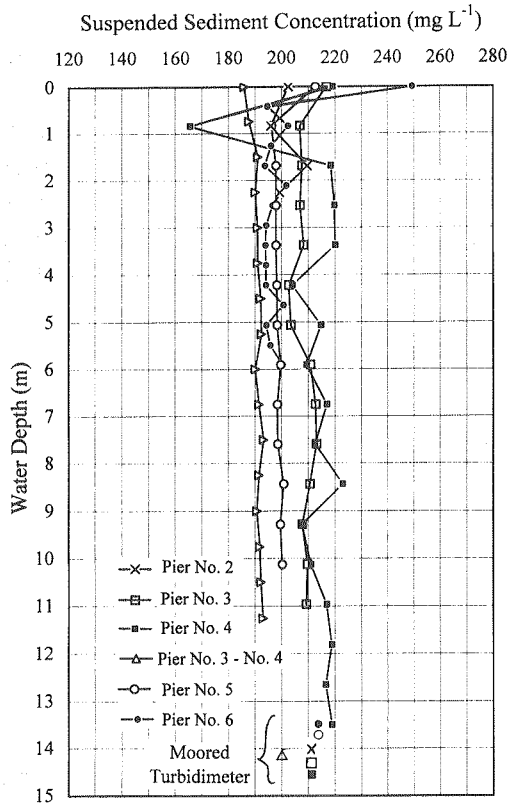

Fig. 5. Vertical distributions of suspended sediment concentration (SSC) in transect of site YKB. Water turbidity (here, equal to SSC) simultaneously recorded by a moored turbidimeter is plotted.

Figure 5 shows vertical SSC profiles at 6 points in transect of site YKB on 22 and 23 June, and corresponding SSC values from the moored turbidimeter. These profiles were obtained downstream of 5 piers of a bridge. It is noted that with an error of less than 15 mg/L, recorded water turbidity (or SSC) is equivalent to vertical SSC downstream of Pier No. 3, Pier No. 4, and their midpoint (open square, solid square, and open triangle in Fig. 5, respectively) rather than at Pier Nos. 2, 5, and 6 near the bank. Including the low SSC near either bank, the recorded turbidity represents the crosssectional SSC with an error of less than 20 mg/L. The great fluctuation at depths of less than 1 m of Pier No. 4 is probably due to the passage of a large organic matter afloat. In fact, we frequently saw trees floating down the river.

3.2 *Characteristics of sediment discharge*

Using water discharge, Q, in m^3/s by U.S. Geological Survey and cross-sectional suspended sediment concentration, C, in kg/m^3 from the moored turbidimeter, we can numerically obtain sediment discharge, Q_s, in kg/s of Yukon River by Equation (1), since the observation error, <20 mg/L, of water turbidity is small:

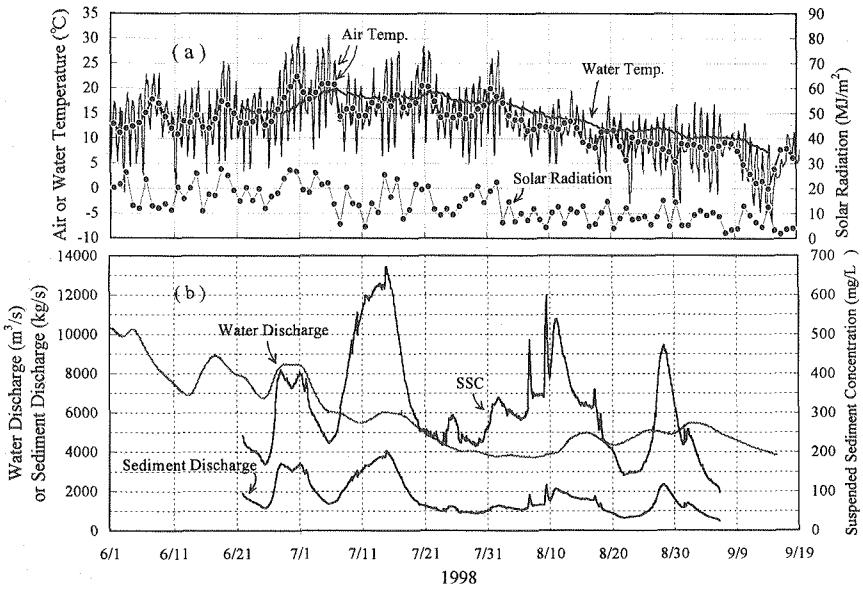

Fig. 6. Time series of (a) air temperature (hourly and daily mean), daily cumulative solar radiation and water temperature, and (b) suspended sediment concentration (SSC), water discharge and sediment discharge at site YKB.

$$Q_s = Q \cdot C. \quad (1)$$

Figure 6 shows time series of (a) air temperature (hourly and daily mean), daily cumulative solar radiation and water temperature, and (b) water discharge, suspended sediment concentration (SSC), and sediment discharge at site YKB. SSC temporally varied in phase with water discharge for a period of 21 June to 5 July, which corresponds to variations of daily mean air temperature and cumulative solar radiation with a time delay of about 11 days. Meanwhile, the water discharge increased abruptly between site YKB and site EAG (see Fig. 7). These suggest that snowmelt in the highland and lowland regions upstream of site YKB increased water discharge and consequently SSC by fluvial entrainment of bank sediment (Chikita, 1996). Thereafter, however, SSC fluctuated greatly, irrespective of decreasing water discharge at site YKB, but corresponding to variations of daily mean air-temperature at sites YKB, ARV (Arctic Village, 636 m asl) and TAN (Tanana, 67 m asl) with a delay of 8 to 11 days (see Fig. 1 for location). Meanwhile, water temperature decreased slightly with abruptly increasing SSC (Fig. 6). The SSC variation independent of water discharge suggests that glacier-melt runoffs with high SSC but relatively very small water discharge were produced consistently from Wrangell Mountains

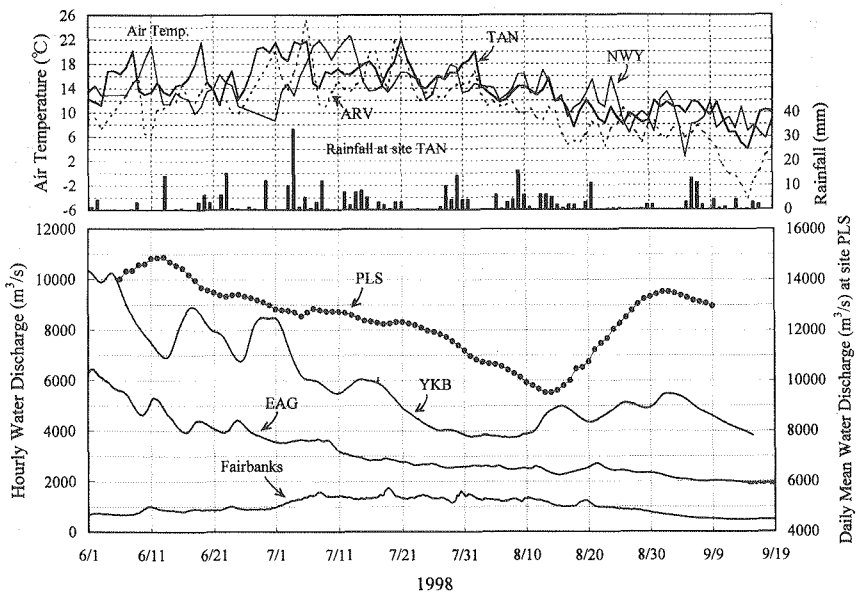

Fig. 7. Meteorology at sites TAN, ARV and NWY, and water discharge at Fairbanks, site YKB, site EAG and site PLS.

and St. Elias Mountains upstream of site EAG (Fig. 1). In fact, water discharge of Tanana River with the relatively large glacier-covered area increased from 1 July, due to glacier-melt discharge possibly with very high SSC (Fig. 7; see Chikita et al, 1998).

Water discharge at site YKB decreased from 1 July through 8 August, and then increased gradually until 1 September (Fig. 6). The gradual increase of water discharge at site YKB from 9 August appears to have occurred with a response to rainfall at site TAN with a delay of about 9 days (Fig. 7). Comparison of water discharge and meteorology in Fig. 7 indicates that the Yukon River water is recharged by snowmelt runoffs in spring or glacier-melt and rainfall runoffs in summer in the lowland and highland regions, including the Brooks Range (see Fig. 1). Meanwhile, sediment discharge at site YKB seems to be produced by snowmelt in the lowland and highland regions until early July, subsequent glacier-melt in Wrangell Mountains and St. Elias Mountains in July to mid August, and glacier-melt plus rainfall in the overall drainage basin through early September. High water discharge at site YKB was induced by snowmelt runoffs, but sediment discharge, the product of water discharge and SSC, reached the maximum on 14 July in the early glacier-melt season, which is due to an abrupt increase of SSC corresponding to the maximum air temperature on 6 July at sites ARV, TAN and YKB.

As shown by plots in Fig. 7, water discharge at site PLS decreased smoothly in the snowmelt and glacier-melt seasons, but increased rapidly from mid August with a response to rainfall. This is probably due to a quick response of tributaries to rainfall events in the lowland and highland regions, because the ground ice in the permafrost regions prevents rainwater from percolating into the underground.

Figure 8 shows a hysteresis between water discharge, x, and SSC, y, at site YKB, plotted every 2 h. Their close relation in the snowmelt-runoff period of 2000 h 21 June to 1800 h 5 July is given by a regression line, $y=2.72\times10^{-7}(x)^{2.322}$. The value of power, 2.322 is nearly equal to 2.111 in case of bank sediment erosion by snowmelt runoffs and to 2.1961 in case of subglacial sediment erosion by glacier-melt, which Chikita (1996) and Chikita et al. (1998) obtained in Ikushunbetsu River, Japan and Peyto Creek, Canada, respectively (Fig. 9). In fact, as shown later, suspended and bank sediments of Yukon River mostly consist of silt and clay as those of Ikushunbetsu River and Peyto Creek. Fluvial entrainment of fine bank sediment by snowmelt runoffs thus seems to prevail upstream of site YKB; ice-melt sediment discharge from the glacial region then possibly did not occur noticeably upstream of site EAG, as shown by small water

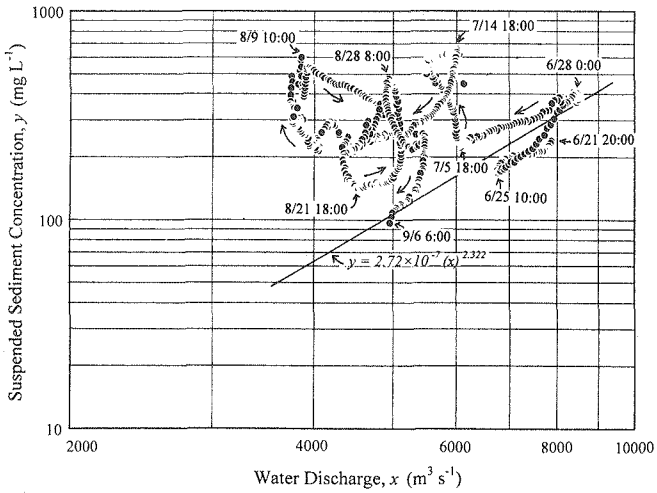

Fig. 8. Hysteresis of water discharge and suspended sediment concentration at site YKB.

discharge of Tanana River with relatively large glacier cover (Fig. 7). Hence, it is suggested that for sediment discharge of Yukon River in the snowmelt season, the bank-sediment erosion prevails under condition that the bottom shear stress, τ_b, or the bank shear stress, τ_L, of river flow is proportional to the sediment amount, M, eroded per unit area per unit time, i.e., $\tau_b \propto \tau_L \propto M$ (Chikita et al., 1998). τ_b is here defined by Equation (2):

$$\tau_b = \rho g R I = \rho u_*^2, \tag{2}$$

where ρ is the water density, g is the gravitational acceleration, R is the hydraulic radius, I is the bottom slope, and u_* is the friction velocity. The coefficient, 2.72×10^{-7} of the regression line in Fig. 8 is much smaller than 4.2762 and 7.8065 in Fig. 9. This indicates that the *sediment availability*, i.e., the sediment amount to be eroded, is relatively very small in Yukon River, compared with the magnitude of the shear stress or water discharge. The proportionality in $\tau_b \propto \tau_L \propto M$ could thus be different in each river. The sediment availability is the highest in Peyto Creek, where much fine sediment is yielded as ground moraine by glaciation. Of all tributaries of Yukon River, Tanana River in glacier-melt runoffs could have the highest SSC because of the largest glacier cover.

Figure 10 shows time series of suspended sediment concentration (SSC), water temperature, and air temperature at site PLS for a period of 27 to 28 June. For comparison, the records at site YKB for 21 to 28 June or 29 June are also

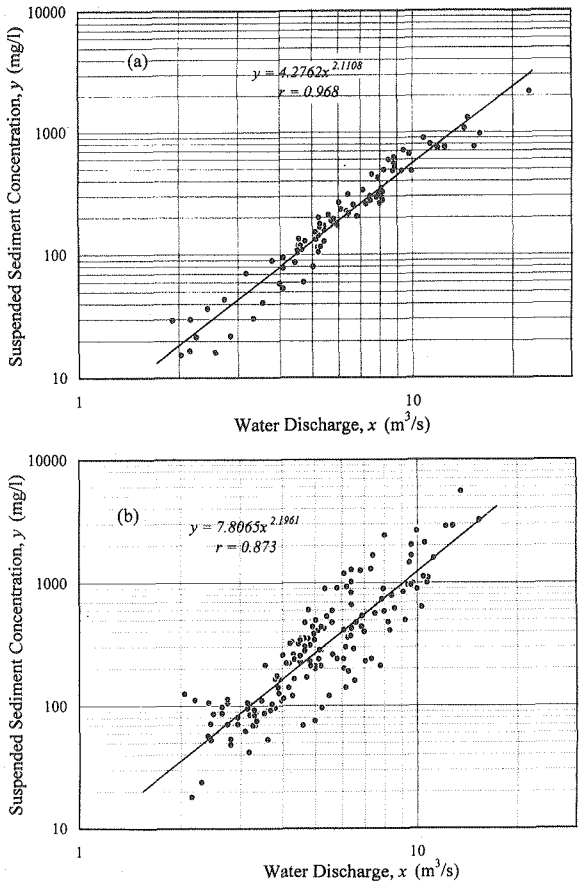

Fig. 9. Relations between water discharge and suspended sediment concentration in (a) Ikushunbetsu River, Japan and (b) Peyto Creek, Canada (Chikita et al., 1998).

shown. The SSC and water temperature at site PLS varied diurnally. A diurnal variation of water temperature occurred also at site YKB almost in phase of that at site PLS, but a diurnal variation of SSC was not observed at site YKB. This suggests that SSC at site PLS was then dominated by snowmelt sediment runoff of local tributaries between site YKB and site PLS, probably exhibiting diurnal variations in both water discharge and SSC as in Ikushunbetsu River (Chikita, 1996). The similar trend in variations of water and air temperatures and solar radiation at site YKB (Fig. 6) indicates that water temperature of Yukon River could be basically controlled by the local heat balance dominated by solar radiation and air temperature except the large

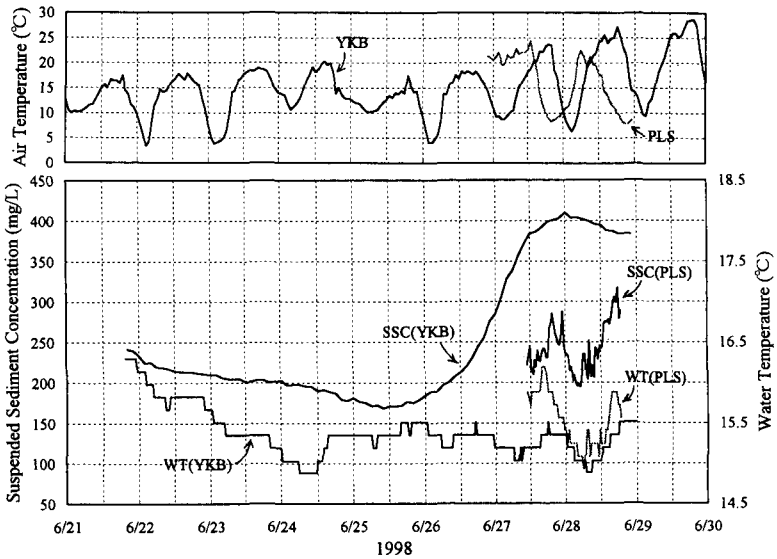

Fig. 10. Time series of air temperature, suspended sediment concentration (SSC) and water temperature (WT) at sites PLS and YKB.

advective heat transport of tributaries during snowmelt runoffs.

3.3 Grain size of suspended and bank sediments

Figure 11 shows cumulative grain size distributions of suspended sediment obtained at (a) site YKB and (b) site PLS, plotted on lognormal probability paper. As shown by lognormal lines, the grain size distributions of suspended sediment are nearly lognormal. The suspended sediment at site YKB consists of 4 to 20 % sand ($\phi \leqq 4$ or $d \geqq 62.5\ \mu$m), 66 to 70% silt ($4 < \phi \leqq 8$ or $62.5 > d \geqq 3.91\ \mu$m), and 10 to 30% clay ($\phi > 8$ or $d < 3.91\ \mu$m), while that at site PLS is relatively fine, composed of 0.1 to 6% sand, 47 to 76% silt, and 18 to 60% clay. Their mean size ranges from 5.6 to 7.1 in phi scale (or from 7.3 to 20.6 in μm) and from 6.6 to 8.3 in phi scale (or from 3.2 to 10.3 in μm), respectively. A relation between d in μm and ϕ in phi scale for grain size is here given by $\phi = -\log_2(d \times 10^{-3})$. The very small grain size of suspended sediment indicates that it is not the bed-material load but the washload originated from the drainage basin including the riverbank. The washload could be produced from the drainage basin during increasing water discharge or fluvial shear stress. This condition is common to that in Ikushunbetsu River and Peyto Creek, which is produced by fluvial entrainment of weathered mineral soil on the riverbank of bedrock in the snowmelt season and by that of subglacial ground moraine in the

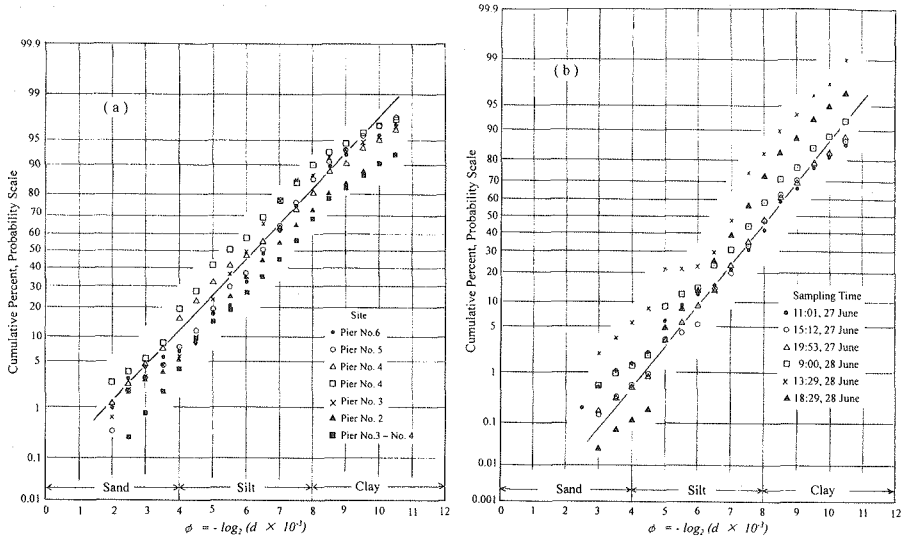

Fig. 11. Grain size distributions of suspended sediment at (a) site YKB and (b) site PLS, plotted on lognormal probability paper.

glacier-melt season, respectively (Chikita, 1996). Yukon River flows in alluvial plains formed in the lowland region for various periods, and its bank sediment consists of fluvial deposits, angular bedrock fragments and their mixture. The fine suspended sediment in the snowmelt season could be supplied by fluvial entrainment of relatively new (unconsolidated) bank deposits.

Figure 12 shows cumulative grain size distributions of suspended sediment (a) at Pier No. 4 of site YKB and (b) at 1953 h 27 June of site PLS (open triangles in Fig. 8), divided into lognormal subpopulations (see Chikita, 1996 for the graphic method). These grain size distributions are nearly lognormal, but, more strictly, can be divided into four lognormal subpopulations, each of which has different phi values of mean, μ, and standard deviation, σ, and a different proportion in weight percent. As a result, at site YKB, suspended sediment consists of a sand-range subpopulation with 10.2%, two silt-range ones with 34.1% and 45.5%, and a clay-range one with 10.3%, and at site PLS, a sand-silt-range subpopulation with 1.8%, two silt-range ones with 16.0% and 34.2%, and a clay-range one with 48.0%. A dotted line in Fig. 12 was made up by the four subpopulations, well reproducing the original cumulative distributions.

Figure 13 shows cumulative grain size distributions of bank sediment at (a) site YKB and (b) site PLS, sampled on 22 and 27 June, respectively, and their partition into some subpopulations. The bank sediments were probably de-

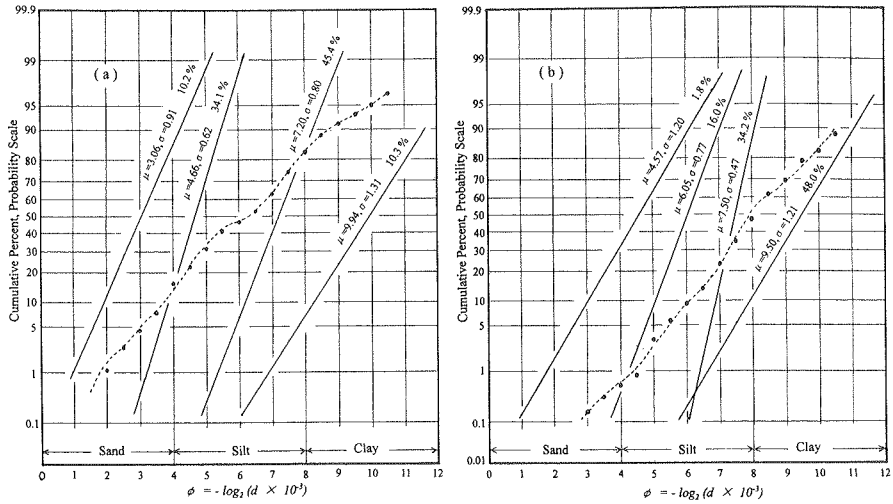

Fig. 12. Grain size distributions of suspended sediment at (a) site YKB and (b) site PLS, divided into four lognormal subpopulations (for sediment of open triangles in Fig. 11). The μ, σ and percentage indicate the mean and standard deviation in phi scale, and proportion in weight percent for each subpopulation, respectively.

posited in the glacier-melt season of the previous year. As a result, the bank sediment can be divided into five and four lognormal subpopulations at site YKB and site PLS, respectively. The two finest subpopulations of bank sediment at site YKB has μ values of 7.54 and 9.79 and σ values of 0.57 and 1.41, which are nearly equal to μ values of 7.50 and 9.50 and σ values of 0.47 and 1.21 for the two finest subpopulations of suspended sediment at site PLS (Fig. 12b). Hence, 82.2% of the suspended sediment at site PLS, equivalent to the total proportion of the two subpopulations, is judged to have been supplied by erosion of bank sediment in the upstream.

4. Conclusions

Water turbidity by a turbidimeter of back-scattering type, deployed in Yukon River, exhibited a one-to-one correspondence to suspended sediment concentration (SSC) of river water. A difference between one-point recorded water turbidity (equal to SSC) and vertical SSC is less than 20 mg/L in transect of the river. Hence, a time series of sediment discharge was obtained, using the turbidity record and the water discharge data. As a result, sediment discharge in Yukon River proved to vary seasonally, exhibiting high water discharge and

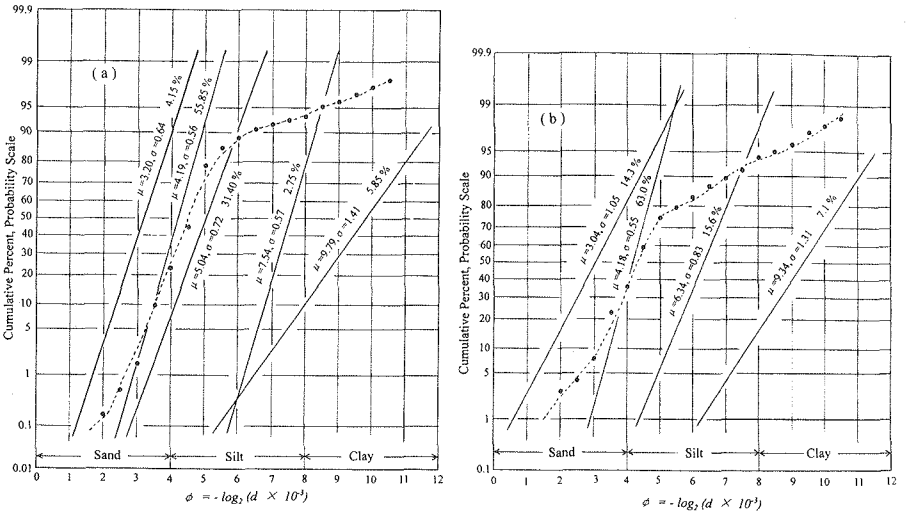

Fig. 13. Grain size distributions of bank sediment at (a) site YKB and (b) site PLS divided into five and four lognormal subpopulations, respectively.

high SSC by snowmelt, and low water discharge and very high SSC by glacier-melt and rainfall.

Information about water turbidity and temperature at other sites, especially site PLS and Fairbanks, in addition to site YKB, is necessary for clarifying sediment discharging processes in Yukon River and its drainage basin.

Acknowledgments

We are grateful to Mr. Carl Pfisterer and Ms. Susanne L. Maxwell, Department of Fish and Game, State of Alaska for their welcome data supply. We are also indebted to Dr. Larry Hinzman, University of Alaska at Fairbanks, for his helpful comments about sediment discharge of Yukon River. Mr. Jack Schmid and Mr. Nobuyuki Sentoh gave us a great help in the field survey. This study was financially supported as part of the Yukon Water & Energy Budget Experiment (YuWEX) Project (supervisor, Dr. Nobuyoshi Ishikawa, Institute of Low Temperature Science, Hokkaido University), Japan Marine Science and Technology Center.

References

Burrows, R.L., W.W. Emmett and B. Parks, 1981. Sediment Transport in the Tanana River near Fairbanks, Alaska, 1977-79. U.S. Geological Survey, Water-Resources Investigations 81-20, 56 pp.

Chikita, K., 1996. Suspended sediment discharge from snowmelt: Ikushunbetsu River, Hokkaido, Japan. Jour. Hydrol., **186**, 295-313.

Chikita, K., Y. Nakamichi, N.D. Smith and M. Perez-Arlucea, 1998. A comparative study on suspended sediment discharge of rivers. Geophys. Bull. Hokkaido University, No. 61, 1-9.

Clifford, N.J., K.S. Richards, R.A. Brown and S.N. Lane, 1995. Laboratory and field assessment of an infrared turbidity probe and its response to particle size and variation in suspended sediment concentration. Hydrol. Sci. Jour., **40**, 771-791.

Harrold, P.E. and R.L. Burrows, 1983. Sediment transport in the Tanana River near Fairbanks, Alaska, 1982. Water-Resources Investigations Report 83-4213, 53 pp.

Jha, R., S. Herath and K. Musiaki, 1998. Application of IIS distributed hydrological model (IISDHM) in Nakhon Sawan catchment, Thailand. Ann. Jour. Hydraul. Engng., JSCE, **42**, 145-150.

Liston, G.E., Y.C. Sud and E.F. Wood, 1994. Evaluating GCM land surface hydrology parameterization by computing river discharge using a runoff routing model: Application to the Mississippi basin. Jour. Appl. Meteorol., **33**, 394-405.

Riley, S.J., 1998. The sediment concentration-turbidity relation: its value in monitoring at Ranger Uranium Mine, Northern Territory, Australia. Catena, **32**, 1-14.